Ignition and Combustion of Boron in O_2/Inert Atmospheres

G. MOHAN* AND F. A. WILLIAMS†
University of California, San Diego, La Jolla, Calif.

From high-speed photographs of the ignition and combustion of laser-ignited boron particles in the 100-μ-diam range, hypotheses are developed concerning ignition and combustion mechanisms for boron. Experimental observations include long periods of one-sided, low-temperature burning for crystalline boron and almost explosive combustion for amorphous boron. An oxide-coating model is developed for describing the low-temperature combustion stage and ignition phenomena. A droplet-burning model is applied to the high-temperature combustion stage. Agreement between theory and experiment is acceptable over a reasonably wide range of conditions.

1. Introduction

CURRENTLY, studies of boron combustion are of practical interest in connection with air augmentation of solid-propellant rockets. Moreover, the complex interplay among the processes of vaporization, conductive and radiative heat transfer, diffusion, chemical reaction, and product condensation, which occur during the burning of boron, imparts an intrinsic interest to such investigations.

The earliest observations on boron combustion are those of Talley,[1] who measured, among other things, rates of oxygen consumption for boron rods, 1 mm in diam, electrically heated to temperatures between 1500°K and 2300°K, at atmospheric pressure. Talley concluded that under these conditions the burning rate was controlled by the outward diffusion rate of $B_2O_3(g)$, which maintained equilibrium with a liquid layer of B_2O_3, perhaps 10μ thick, that coated the boron rod.

The previous experimental study that resembles the present work most closely is the time-exposure photography of falling particles in the 177-μ to 250-μ-diam range, ignited by a xenon flash, in air and in oxygen-argon mixtures of various concentrations, at atmospheric pressure, as reported by Prentice.[2] A two-stage combustion process was observed; the first, low-temperature stage was presumed to correspond to a surface-burning process and the second, high-temperature stage to gas-phase combustion. Periodic intensity variations of the streaks were sometimes evident in the low-temperature stage, and the color temperature of the particle was observed to increase with time, except near the flammability limit (about 9% mole fraction of oxygen in argon) where the second stage disappeared.

Macek and Semple[3] ignited boron particles, approximately 40μ in diam, at atmospheric pressure in hot (2200°K to 2900°K) oxidizing gases of various compositions, produced in a specially designed gas burner. In addition to verifying the existence of the two-stage combustion mechanism, they obtained burning times for each stage from time-exposed photographs. Both burning times were found to be inversely proportional to the mole fraction of oxygen. An ignition temperature for the particle of approximately 1950°K was obtained.

Knipe[4] proposed three quasi-steady diffusion-controlled combustion models, to consider the effects of gas-phase and surface chemical equilibria and to account for condensed oxide, either as a liquid film on the particle surface or as a fog detached from the particle surface. The equilibrium model, believed to be most nearly applicable for high-temperature combustion, predicts that the primary constituent leaving the boron surface is $B_2O_2(g)$, generated through oxidation of B(l) by $B_2O_3(g)$, which has been produced in a gas-phase flame that contains appreciable concentrations of $BO_2(g)$ and that exhibits reactions whose over-all effect is oxidation of $B_2O_2(g)$ by $O_2(g)$.

Recently, Macek and Semple[5] ignited boron particles 75 μ in diameter by dropping them through the focused beam of a continuous CO_2 laser, in air and in 20/80 oxygen-argon mixtures, at pressures from 1 to 35 atm. From time-exposed photographs taken through a stroboscopic disk, burning times for each of the two combustion stages were obtained under room-temperature environmental conditions. It was found that whereas the duration of the high-temperature stage was reasonably reproducible, the duration of the low-temperature stage was highly nonreproducible at pressures above approximately 10 atm; at 35 atm in O_2/Ar, times from 6 to 113 msec were observed for the first stage.

More recently, King[6] defined and analyzed a model for the low-temperature combustion stage, assuming a spherically symmetrical, transient system with a liquid oxide film on the boron particle. It was presumed that oxide production is controlled by diffusion of oxygen through the liquid film and that kinetically controlled vaporization of B_2O_3 occurs at the liquid-gas interface. The nonlinear ordinary differential equations describing the model were integrated numerically for a wide variety of conditions. Predictions concerning both the ignition temperature and the burning time in the low-temperature stage were drawn from the numerical results.

The objective of the experimental work reported here is to shed more light on the combustion processes described above. By igniting individual boron particles with a pulsed laser, we establish an initial condition of incipient ignition that is affected minimally by the relative flow of gas. By observing the particle with high-speed motion-picture photography as it burns, we can interpret more easily the character of the combustion process. The experimental apparatus is described in the following section. Next, qualitative experimental observations on the combustion of both granular and amorphous boron are presented. In subsequent sections, theoretical considerations pertaining mostly to the low-temperature stage of combustion are developed. It will be

Received August 9, 1971; revision received January 17, 1972. These studies have been supported under Project THEMIS and were sponsored by the Air Force Office of Scientific Research, Office of Aerospace Research, United States Air Force, under Contract F44620-68-C-0010. We acknowledge interesting communications from A. Gordon, M. King, R. Knipe, A. Macek and J. Prentice.

Index category: Combustion in Heterogeneous Media.

* Research Assistant, Department of Aerospace and Mechanical Engineering Sciences.

† Professor of Aerospace Engineering, Department of Aerospace and Mechanical Engineering Sciences. Associate Fellow AIAA.

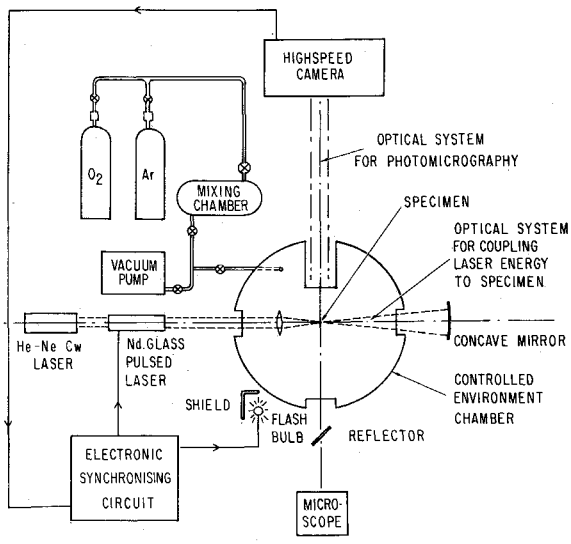

Fig. 1 Schematic diagram of the experimental apparatus.

seen that the observations can be understood within a coherent framework.

2. Experimental Technique

The apparatus employed here is basically the same as that developed by Wilson[7] for studying the combustion of aluminum. The arrangement is sketched in Fig. 1. In this work, results are reported for two types of specimens, crystalline granules of boron, (supplied by J. Prentice, Naval Weapons Center, China Lake, Calif., in the size ranges 62–74 μ, 74–88 μ and 88–105 μ) and amorphous boron (obtained from L. Edwards, Wright-Patterson Air Force Base, Ohio).

A roughly spherical boron particle of 50 to 150 μ diam is held at the tip of a 10μ glass fiber by natural adhesive forces. The particle is ignited by the radiative flux of a commercial neodymium-doped glass laser (American Optical Co., Model: Uni-Laser Mark II), which uses a $\frac{3}{4} \times 6\frac{5}{8}$ in. rod and is air-cooled. The beam diameter is 3 mm and typical beam divergence is 90 mr, full-angle half-energy. The laser is rated to deliver up to 1 joule at a wavelength of 1.06 μ, in a 600 μsec pulse. The stimulated emission is focused onto the surface of the boron particle by a convex lens of 6.5 cm focal length and a concave mirror of 13 cm radius of curvature. The purpose of the mirror is to equalize, approximately, the fluxes incident on opposite sides of the particle, thereby preventing the particle from moving rapidly out of the field of view under the impulse of the vapors expelled from the particle during irradiation. During ignition, the particle separates from the glass fiber, and the tip of the fiber often melts and contracts under its surface tension. The suspension device therefore usually does not interfere with the combustion process.

The particle is aligned for the pulsed-laser beam using a continuous He-Ne Laser (Quantum Physics LS-32; 2 Mw). The continuous beam passes through the mirrors of the Nd-glass laser. The alignment is perfected by using carbon paper as a target at the focal point of the lens. The particle can then be positioned in the continuous laser beam, by using an x-y traverse, integral with the support system. The initial particle size is measured with 25 μ accuracy by the eyepiece scale in the microscope.

The ignition and combustion of boron particles were recorded by a 16-mm Hycam high-speed camera, at measured framing rates typically of 5000 fps. Sensitive Kodak RAR 2479 negative film was used, with an aperture of f/16 and a magnification factor of 6 on the film. Backlighting was provided by ordinary flash bulb (AG-1B General Electric), in conjunction with a reflector.

Since the particle is suspended in a closed chamber, the pressure and composition of the oxidizing environment could be set at will, within the design restriction that the pressure not exceed 10 atm. Either air or mixtures of oxygen with argon (commercial grade O_2 with 0.5% impurities and high-purity dry grade Ar, 99.996% pure, both supplied by Linde Division, Union Carbide Company), typically 20/80 and 50/50 mole ratios, were used as the environment in the present tests. The pressure setting ranged from 0.75 atm to 1.5 atm. The chamber was evacuated to 1 cm of Hg by a reciprocating vacuum pump and charged with the mixture from the mixing chamber. Results will be shown here only for environments of atmospheric room-temperature air, because over the range of conditions investigated the observed phenomena of ignition and combustion were affected little by changes in the environment.

Laser discharge was synchronized electronically with the flash bulb. At the desired setting on the footage scale in the camera, the event-synchronizer switch triggers the electronic circuit, which initiates the flash bulb and fires the laser after the time delay (0.01–100 msec) set on the pulse generator.

3. Experimental Observations for Granular Boron

The studies reported in Refs. 1–6 were all concerned with granular boron. We have found that granular boron is relatively difficult to ignite at atmospheric conditions. A variety of different particle histories were observed to occur subsequent to the laser pulse, under essentially the same conditions. Yet, we have not seen the second (high-temperature) stage of combustion, even though in some cases we have followed the particle for 40 msec after the pulse. We believe that in many of the runs the high-temperature stage occurs after the particle moves out of the field of view of the camera. The types of behavior that we have observed are illustrated in Figs. 2–4.

At low laser energy inputs the particle remained attached to the probe, did not ignite, and cooled from incandescence in less than 1 msec. At higher energies, phenomena such as that shown in Fig. 2 occur. The line extending downward is the glass probe that supports the particle prior to ignition. In this and every other sequence shown herein, we believe that the laser energy incident from the right slightly exceeds that incident from the left. In the first frame, the probe and the particle both glow in the laser light. The particle is oblong (as are most boron granules), with length and width of roughly 150 and 30μ, respectively. It is seen that as the particle

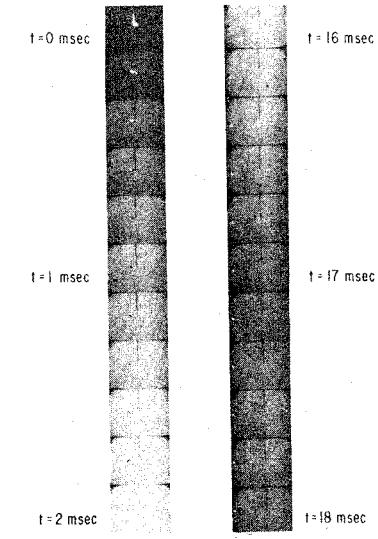

Fig. 2 Combustion of crystalline boron particle, approximately 150μ by 30μ, in air at 300°K and 1 atm, with low-intensity back-lighting; 5 frames/msec; moderately low ignition stimulus.

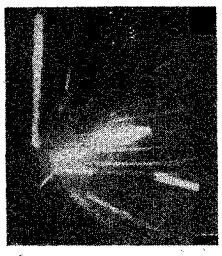

Fig. 3 Combustion of crystalline boron particle, 120μ in diam, in air at 300°K and 1 atm, with no backlighting; 5 frames/msec; moderately high ignition stimulus.

detaches itself from the probe, approximately half of it ceases to glow. In this case, one-sided burning continues for more than 30 msec, and the particle spins at approximately 250 rps. One-sided burning of this kind was observed in a number of runs. Spin rates were reasonably uniform during a run but variable from run to run; spin appeared to be associated mainly with initial conditions and not influenced greatly by asymmetric vapor emission during combustion. Surface burning appears to occur and to involve a low rate of expulsion of hot oxide vapor and probably also diffusion through a liquid oxide puddle. On the basis of these results, we would ascribe the periodic intensity variations, evident in some of the particle streaks in the time exposures of Prentice,[2] to one-sided burning and spin during the first stage of combustion.

A nonbacklighted sequence for a nearly spherical particle, 120μ in diameter, that receives a high energy input is shown in Fig. 3. The first two frames suggest thorough oxide melting. The establishment (frame 3) in less than 0.2 msec of an extensive gas-phase zone of hot oxide indicates appreciable oxide vaporization, with associated entrainment and ejection of liquid oxide. It seems likely that some melting of the boron occurs, since its melting point (2450°K) does not greatly exceed the normal boiling point (2316°K) of the oxide. However, the inrush of O_2 to react with the exposed hot boron carries the B_2O_3(l) fog back to the surface of the particle in about 0.5 msec (frames 4 and 5). Thereafter, a milder surface reaction persists over the entire surface of the particle, as can be seen for the final 0.6 msec in Fig. 3. This type of burning continued for at least 3 msec, at which time the particle left the field of view. Since liquid oxide can remain on the boron particle only if its surface temperature is below the boiling point of the oxide, any melted boron must resolidify before the mild surface burning involving diffusion through an oxide film can occur; the slightly nonspherical shape of the hot particle, particularly evident in later frames, supports the contention that the boron is solid. On the basis of the work of Macek and Semple,[5] for example, we expect that eventually all of the boron will melt, and an extended gas-phase reaction zone will be established. However, the low-temperature "self-cooking" period apparently quite generally precedes this second reaction stage.

The single nonbacklighted frame shown in Fig. 4 indicates the peculiar behavior that can occur when the laser energy is distributed unevenly over the surface of the particle. The vertical line is the hot probe attached to a cold portion of the 100μ particle, and the other streaks represent burning portions of the particle, up to 5μ in diameter, which have been ejected as a consequence of the extreme local heating caused by energy nonuniformity and by surface irregularity. Similar photographs with backlighting reveal that although this type of heating produces large forces on the particle, it seldom leads to either sustained combustion or consumption of an appreciable fraction of the boron.

4. Experimental Observations for Amorphous Boron

The two frames shown in Fig. 5 demonstrate what happens when an amorphous boron particle is irradiated by the laser at atmospheric conditions. The particle was approximately spherical and 150μ in diameter. Violent combustion occurs in the first frame; in the second, 0.2 msec later, only the hot probe and a few of the larger burning fragments remain visible. Backlighted photography for amorphous boron has shown clearly that essentially complete combusion is achieved, always within 1 msec. Moreover, the ejected fragments often appear to exhibit the two-stage burning mechanism noted by earlier investigators, but on a much shorter time scale, as might be expected from their much smaller size.

This type of behavior can be understood if one realizes that the "amorphous" boron particles are in fact agglomerates of very small particles, typically in the submicron size range. The exceedingly large specific surface area leads to efficient in-depth

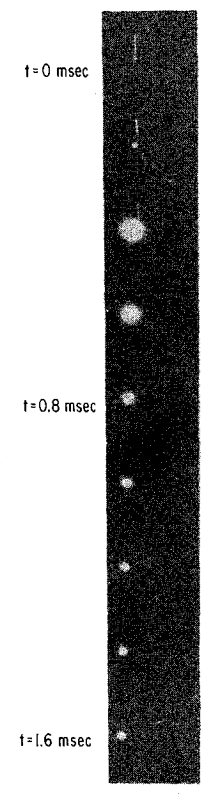

Fig. 4 Fragmentation of crystalline boron of diam 100μ in ambient air.

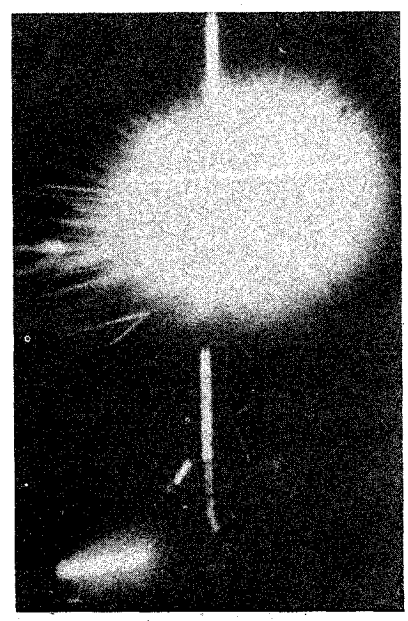

Fig. 5 Laser-ignited amorphous boron of diam 150μ at 1 atm, 300°K, ambient air.

absorption of the laser energy, and the resulting heating of entrapped gases rapidly propels hot fragments outward, distributing them into oxygen-rich gas regions, where they are consumed in the submillisecond burning times of submicron particles. In this respect, for amorphous boron, radiant ignition is much more efficient than hot-gas ignition, whereas the reverse may be true for granular boron, because it is so difficult to raise the temperature of a larger boron crystal.

5. Comparison with Aluminum

The character of the low-temperature combustion stage and our inability to bypass this stage experimentally require explanation. In particular, nonreproducibility of the duration of this stage[5] and our observations of one-sided burning should be considered. The rest of this paper details our attempts to develop theoretical explanations.

At first glance, one-sidedness may not seem unusual, since oxide cap formation on burning aluminum droplets is a well-known phenomenon.[7] However, the mechanism of the process for boron cannot be the same as that for aluminum. Since the vapor pressure for Al exceeds that for Al_2O_3, it is clear that an oxide cap can sit on one side of an isothermal aluminum droplet while the other side vaporizes under energy input from a gas-phase combustion zone. The process perpetuates the asymmetry. On the other hand, for boron the vapor pressure of the oxide is the greater. Therefore under isothermal conditions B_2O_3 is expected to vaporize more rapidly, and the mechanism operative for aluminum cannot sustain itself. One can explain our observations of long periods of one-sided burning by allowing substantial condensed-phase temperature gradients to exist for appreciable lengths of time.

6. Peculiarity of the Thermal Conductivity of Boron

There is a variety of rather unique properties of boron that favor large internal temperature gradients. The crystal structure of boron is relatively complex, there being a rhombohedral form at room temperature, a tetragonal form and perhaps four or five other forms between 1000°K and 1500°K, and a second rhombohedral form above 1500°K.[8] Although a given crystal may not pass through all of these forms during heating, nevertheless the heat capacity of boron is relatively high, its average value between room temperature and the melting point being approximately 0.6 cal/g.[9]

Probably of greater importance is the remarkably low thermal conductivity of solid boron at high temperatures. Its relatively high Debye temperature (1219°K), accompanied by a large contribution to the thermal resistivity from umklapp scattering[10] (two-phonon scattering in an anharmonic potential without momentum conservation, a process whose existence has been verified only for three or four materials) produces a thermal diffusivity that decreases sharply with increasing temperature, reaching a value of $\alpha = 5 \times 10^{-3}$ cm^2/sec at 2000°K.[11] This value is an order of magnitude lower than the diffusivity of the condensed phase of any other element of group III at any temperature, more than two orders of magnitude lower than the lowest thermal diffusivity of solid aluminum, and comparable with diffusivities of elements of group VIA, the group with the lowest thermal diffusivities of all elements between room temperature and their normal boiling points.[11] At 2000°K the characteristic heat-conduction time for a boron particle with a characteristic dimension of $d = 100\mu$ is $d^2/\alpha = 20$ msec. A more thorough heat conduction calculation for a semi-infinite solid of boron initially at 300°K, whose surface temperature is instantaneously raised to 2000°K, reveals that a point 100μ from the surface requires approximately 7 msec to reach 723°K, the meling point of B_2O_3. Thus, large temperature gradients clearly can persist for long times within boron particles.

In addition to lending understanding to the one-sided burning phenomenon, these observations help to explain the occurrence of the low-temperature combustion stage. It should be emphasized first that heat-transfer estimates reveal that, in principle, a one-joule laser delivers more than enough energy to heat a particle in the 100μ size range to an average temperature exceeding 2500°K in 0.5 msec, without raising the surface temperature of the particle to a value near the normal boiling point of boron, 3931°K. Hence, unless condensed-phase phase-changes are extremely slow for kinetic reasons, it should be possible to establish directly, in less than 1 msec, the type of quasi-steady gas-phase combustion that will be described in Sec. 12 as being representative of second-stage combustion. Although it appears possible to achieve the required temperature level directly, the calculations that we have just cited in considering one-sided burning suggest that it may be difficult. If boron melting must precede gas-phase burning, then the extraordinarily high heat of fusion of boron (about 500 cal/g)[9] contributes further to the difficulty. Consequently, neither we nor previous investigators have succeeded in producing second-stage combusion directly. For ignition to occur at all in our experiments, it is therefore necessary for a combustion regime to exist at a lower temperature than the particle temperature of Sec. 12. Since the boiling point of B_2O_3 is not far below 2500°K, it seems likely that in this low-temperature combustion regime oxide coats the boron surface, and some type of surface-burning mechanism must operate.

7. Combustion Model for the Low-Temperature Stage

A reasonable model for the combustion mechanism in the low-temperature stage is illustrated schematically in Fig. 6. The layer of B_2O_3(l) is thin enough to be treated as a planar slab bounded by solid boron at B and by the ambient gas at C. The over-all reaction that occurs is $2B(s)+\frac{3}{2}O_2(g) \rightarrow B_2O_3(g)$. At B, a diffusion-controlled reaction of O_2 with B produces B_2O_3(l) and heat. At C, equilibrium vaporization of B_2O_3 and equilibrium absorption of O_2 occur. As an alternative model it would be possible to assume that the reaction at B is the energetically nearly neutral process $nB_2O_3+nB \rightarrow 3B_nO_n$ and that the exothermic process $2B_nO_n+(n/2)O_2 \rightarrow nB_2O_3$ occurs either at C or at a liquid-phase diffusion flame located somewhere between B and C, but the results would not differ greatly from those of the adopted model. Since no information is available concerning solubilities and diffusion coefficients of O_2 and of suboxides in B_2O_3(l), we have selected the simplest combustion mechanism. This model is very similar to that of King,[6] although each was developed independently. Essentially the only differences are planar vs spherical symmetry and equilibrium vs rate-controlled vaporization of B_2O_3.

If the temperature varies over the surface of the particle, then the model illustrated in Fig. 6 is to be applied to the hottest portion of the surface. The combustion will tend to perpetuate itself at the hottest spot for three reasons. First is the slow thermal response discussed in Sec. 6. Second, the rate of oxide vaporization will be greatest at the highest temperature, thereby tending to keep the oxide layer thin. Third, liquid-phase diffusion coefficients typically exhibit an Arrhenius temperature dependence,[12] causing diffusion rates (and hence, within the context of

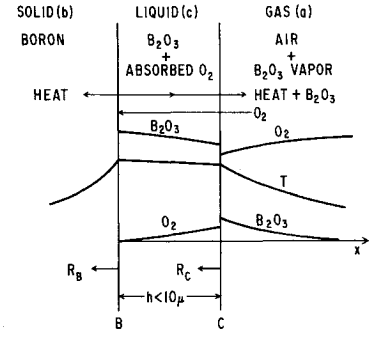

Fig. 6 Model for low-temperature stage in the combustion of boron particles.

the model, heat-release rates) to be greatest at the position of highest temperature.

If the regression rates of the surfaces B and C are R_B and R_C respectively, then the thickness h of the liquid layer obeys the equation

$$dh/dt = R_B - R_C \tag{1}$$

We assume that the thickness and thermal resistivity of the liquid layer are small enough for the layer to be approximately isothermal, and we write an energy balance for the layer in the form

$$h\rho_c c_c dT_c/dt = q_B \rho_b R_B - q_C \rho_c R_C - L \tag{2}$$

where T_c is the temperature of the layer, c_c the heat capacity of B_2O_3(l), ρ_b and ρ_c the densities of B(s) and B_2O_3(l), respectively, q_B the heat liberated per unit mass of boron consumed at B, q_C the heat absorbed per unit mass of B_2O_3 vaporized at C, and L the sum of the heat losses by radiation and conduction. The use of suitable expressions for R_B, R_C and L in Eqs. (1) and (2) will complete the mathematical description of the combustion model.

Hypothesizing absorptive equilibrium for O_2 at C and one-dimensional steady-stage diffusion of O_2 within the liquid layer, with a diffusion-controlled reaction at B, we obtain

$$R_B = XkD/h \tag{3}$$

where X is the mole fraction of O_2 in the ambient atmosphere, k is an effective distribution coefficient related to the ratio of the mole fraction of O_2 absorbed in B_2O_3(l) to the gas-phase mole fraction, and D is the diffusion coefficient for absorbed O_2 in B_2O_3(l). In terms of the distribution ratio k' (the equilibrium ratio of liquid-phase to gas-phase oxygen concentration), which ideally is a function only of the temperature T_c, the quantity k is given by $k = (\frac{4}{3})k' pW_B/(\rho_b R^0 T_c)$, where p is the total ambient pressure, W_B is the atomic weight of boron, and R^0 is the universal gas constant. The factor $\frac{4}{3}$ in this formula (which presumes an ideal gas mixture at C) arises from the stoichiometry of the reaction at B. We note that the product kD is proportional to p and that both k and D must be evaluated at temperature T_c.

Although our principal results would be qualitatively unchanged had we assumed that spherically symmetrical gas-phase diffusion controls the inflow rate of O_2 instead of liquid-phase diffusion, comparison of the straightforwardly calculated gas-phase diffusion rate of O_2 with the observed burning rate in the low-temperature stage strongly suggests that gas-phase diffusion of O_2 is not rate-controlling. On the other hand, as will be discussed more fully in Sec. 11, for R_C outward gas-phase diffusion of B_2O_3(g) is rate-controlling over a wide range of conditions, whence

$$R_C = 2X_a D_a \rho_a/\rho_c d \tag{4}$$

where X_a is the ratio of the equilibrium vapor pressure of B_2O_3 at temperature T_c to the total pressure, d the diameter of the particle, D_a the binary diffusion coefficient of B_2O_3(g) in air at T_c, and ρ_a the density of a pure ideal gas of B_2O_3 at ambient pressure and temperature T_c. The product $\rho_a D_a$, which is independent of p, has been presumed independent of temperature, and X_a has been assumed to be small compared with unity, a reasonable approximation for $T_c < 2100°K$.

For the term L in Eq. (2), under the conditions of interest here, heat losses by inward heat conduction, by outward heat conduction, and by outward radiation are all roughly comparable in magnitude.

8. Stability for the Low-Temperature Stage

A steady-state solution exists for Eqs. (1) and (2) such that

$$R_B = R_C = (q_C \rho_c R_C + L)/q_B \rho_b \tag{5}$$

The stability of this solution can be investigated by linearization about the steady state. To perform the linearization, we must evaluate partial derivatives with respect to both h and T_c at the steady-state conditions. We use the formulas

$$\partial R_B/\partial h = -R_B/h, \quad \partial R_B/\partial T_c = (A/R^0 T_c)(R_B/T_c) \tag{6}$$

$$\partial R_C/\partial h = 0, \quad \partial R_C/\partial T_c = (H/R^0 T_c)(R_C/T_c) \tag{7}$$

$$\partial L/\partial h = 0, \quad \partial L/\partial T_c = dL/dT_c \tag{8}$$

$\rho_c c_c = \text{const}$, $q_B \rho_b = \text{const}$ and $q_C \rho_c = \text{const}$. Equation (6) follows from Eq. (3) under the assumption that at constant pressure the product kD can be expressed in an Arrhenius form, viz., proportional to $\exp(-A/R^0 T_c)$, where A is the difference between the activation energy for diffusion and the heat of absorption. Equation (7) follows from Eq. (4) under the assumptions that $(D_a \rho_a/\rho_c d)$ changes negligibly and that X_a is proportional to $\exp(-H/R^0 T_c)$, where H is the molar heat of evaporation of B_2O_3 at temperature T_c. Equation (8) is a consequence of the character of the heat-loss processes.

The stability analysis is not difficult to perform and reveals that the steady state is stable if and only if both

$$T_c dL/dT_c > LH/R^0 T_c \tag{9}$$

and

$$\frac{H}{R^0 T_c} + \frac{\rho_c c_c T_c}{q_B \rho_b} + \left[T_c \frac{dL}{dT_c} - \frac{LH}{R^0 T_c}\right](q_B \rho_b R_B)^{-1} > \frac{A}{R^0 T_c} \tag{10}$$

Since $H = 87.6$ kcal/mole whereas activation energies for absorption or liquid-phase diffusion seldom exceed 20 kcal/mole, Eq. (10) generally is satisfied whenever Eq. (9) is satisfied. This conclusion is supported further by King's inference that $A = 45.3$ kcal/mole,[6] deduced from unpublished observations by Talley and Henderson concerning the thickness of the oxide layer on electrically heated boron rods at two different temperatures. However, Eq. (9) is not satisfied in the laser-ignition experiments. Hence, the steady surface-burning process that occurs in the low-temperature stage is unstable.

Equation (9) is equivalent to the stability condition encountered in classical thermal ignition theory, where heat loss is balanced against heat generation by an exothermic reaction whose activation energy is H. However, the present analysis has been essentially different from the classical theory, since dynamics associated with time-varying thickness of the liquid layer have been taken into account. The present problem is of the second order, whereas the classical theory describes a first-order problem, and here it is an endothermic process whose activation energy is H.

A closer investigation of numerical values for the parameters appearing in Eq. (9) is of interest in connection with various boron combustion experiments. For $T_c \approx 2000°K$, we find $H/R^0 T_c \approx 20$. In laser-ignition experiments after cessation of the pulse, $d \ln L/d \ln T_c$ is 4 for radiant loss and roughly unity for conductive loss, so that the steady-state condition is always unstable. On the other hand, in the experiments of Talley[1] with electrically heated rods, radiant heat losses are usually more important than conductive heat losses, thereby tending to make dL/dT_c high, and L is small because the temperature-independent electrical energy input provides a negative contribution almost as large as the total loss. Estimates employing Eq. (9) show that in this case the steady-state condition is stable, as was found experimentally.

9. Burning Time for the Low-Temperature Stage

Suppose that laser ignition establishes a state of combustion slightly removed from the steady state. Since the steady state is unstable, extinction will gradually occur if the oxide layer is thicker and the temperature is lower than for the steady condition, whereas acceleration of the burning will occur if the oxide layer is thinner and the temperature is higher. Although the relative importance of deviations in thickness and in temperature is difficult to investigate accurately, it appears from the linearized nondimensional form of Eq. (1) that since the temperature term is multiplied by the large factor $H/R^0 T_c$, temperature deviations will dominate the response. Thus, from Eq. (1), an increase in temperature will cause the thickness of the liquid layer to decrease and a combustion process with a

clean boron surface to develop. A rough estimate of the characteristic time τ for the new combustion regime to appear is h/R_B, the characteristic time associated with the linearized forms of Eqs. (1) and (2). Equation (3) yields

$$\tau = h^2/XkD \tag{11}$$

which can be taken as an estimate of the burning time for the low-temperature stage.

Accurate estimates of h and of kD in Eq. (11) are difficult to obtain. King[6] deduced a value for kD from the Talley-Henderson measurement. His result is roughly in agreement with the physically reasonable estimates $D = 10^{-5}$ cm^2/sec and $k = 10^{-1}p$, with p in atmospheres. Use of these numbers along with the possibly representative value $h = 10^{-4}$ cm gives from Eq. (11) the realistic result that $\tau = 50$ msec in air at atmospheric pressure.

Equation (11) predicts that τ is inversely proportional to X, in agreement with the measurements of Macek and Semple.[3] Another conclusion that can be drawn from Eq. (11) is that the burning time should be strongly dependent upon the ignition stimulus, since this greatly affects the value of h and the extent to which h and the surface temperature differ from their steady-state values. In this respect, there is agreement between the present view and the nonreproducibility of the duration of the low-temperature stage observed by Macek and Semple.[5]

If Eqs. (1) and (2) are linearized, then since the system is of the second order, both oscillatory and exponential solutions might appear. However, the values of the parameters are such that in all cases only exponential solutions occur. Mild nonlinearities that appear in these equations are not expected to alter this qualitatively exponential character substantially. The strong nonlinearity in the Arrhenius terms enhances the growth rate, giving further impetus to an accelerating divergence to the high-temperature stage of combustion. In this respect, the model agrees with qualitative observations of Macek and Semple.[5]

It is more difficult to reconcile with the present viewpoint some of the observations on hot-gas ignition described by Macek and Semple.[3] Since most of their reported gas temperatures exceed the boiling point of the oxide, it appears that conductive heat transfer from the gas to the particle generally occurs during their low-temperature stage of combustion. Moreover, estimates suggest that in most cases the conductive energy input exceeds the radiative energy loss. Under these conditions ($L < 0$), the second equality in Eq. (5) cannot be satisfied, and there exists no steady state about which the equations can be linearized. The distinct lessening in the intensity of the particle track that was observed toward the end of the first combustion stage[3] is also unique. It is possible that transient dynamical behaviour described by Eqs. (1) and (2) would agree with the observations. For example, there may be a temperature range, below the oxide boiling point, where R_B exceeds R_C, so that h tends to increase with time, thereby effecting a reduction in the heat-release rate and explaining the fading of the track. Since R_B increases with X, the reduction would be more pronounced at higher ambient oxygen concentrations, as was observed experimentally. However, in the absence of numerical integrations of Eqs. (1) and (2), these suggestions for explaining the observations of Ref. 3 are speculative at best. The numerical integrations for an alternative model, performed by King[6] and discussed in Sec. 11, do not demonstrate clearly this observed effect.

10. The Ignition Temperature

Since the steady state defined by Eq. (5) divides conditions of accelerated burning from conditions of progressive extinction, an ignition temperature should be derivable from Eq. (5). In fact, the combination of Eq. (4) with the second equality in Eq. (5) yields as the steady-state condition

$$p_e = \left(\frac{R^0 T_c \rho_c}{2D_a W}\right)\left(\frac{Ld}{q_B \rho_b - q_C \rho_c}\right) \tag{12}$$

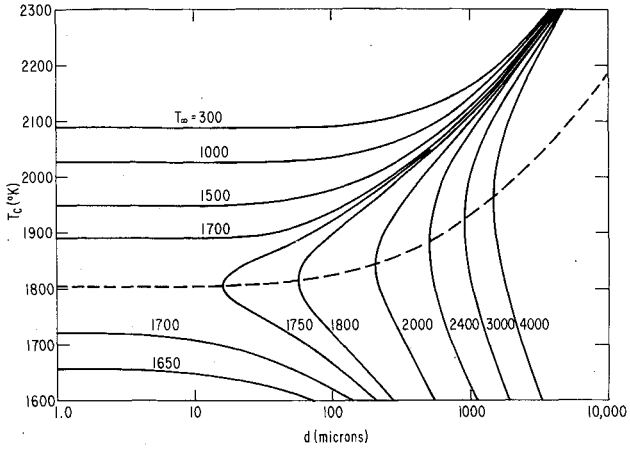

Fig. 7 Effect of particle diameter on the ignition temperature of boron at different ambient temperatures and at atmospheric pressure.

where p_e is the equilibrium vapor pressure of B_2O_3 at temperature T_c, and W denotes the molecular weight of B_2O_3. The solution to Eq. (12) that corresponds to an unstable condition should define the ignition temperature T_c of the particle for laser-ignition experiments. Equation (12) demonstrates explicitly that p_e is predicted to be approximately proportional to the product of the particle diameter with the heat loss per unit surface area of the particle, to be proportional to the ambient pressure, and to be approximately independent of other experimentally adjustable quantities such as ambient oxygen mole fraction. If outward conductive heat losses are dominant (e.g., for small particles in cool atmospheres) then according to Eq. (12) p_e is independent of particle size and proportional to the differences between the particle temperature and the ambient temperature. If radiative heat losses are dominant, then p_e is predicted to be proportional to dT_c^4. That p_e should increase with increasing d for radiative loss is consistent with the fact that Talley[13] found a relatively high ignition temperature, about 2200°K, roughly 250°K above that obtained by Macek and Semple.[3] This difference is approximately that predicted by Eq. (12).

We have employed Eq. (12) to calculate the theoretical ignition-temperature curves at atmospheric pressure, shown in Fig. 7, where the ambient temperature T_∞ and the particle diameter d are the parameters that were varied. The term L was taken to be the sum of outward conductive and radiative losses, viz., $L = (T_c - T_\infty)(2\lambda/d) + 1.36\varepsilon(T_c/1000)^4$. It was assumed that the gas-phase thermal conductivity is $\lambda = 3 \times 10^{-4}$ cal/cm sec °K, that the emissivity of the oxide surface is $\varepsilon = 0.5$, that the diffusion coefficient of B_2O_3(g) through air at 1 atm and 2000°K is $D_a(2000/T_c) = 0.8$ cm^2/sec, that the vapor pressure of B_2O_3 in atmospheres is $p_e = \exp(H/R^0T_b - H/R^0T_c)$ where T_b is the normal boiling point of B_2O_3, and that $\rho_b = 2.35$ g/cm^3, $\rho_c = 2$ g/cm^3, $T_b = 2316$°K, $H = 87.6$ kcal/mole, $q_B = 13.3$ kcal/g and $q_A = 1.26$ kcal/g, as obtained from tables.[9]

Along the dashed line in Fig. 7, the two sides of Eq. (9) are equal. Below the dashed line Eq. (9) is satisfied, and the steady state is stable. If steady burning conditions were established in this low-temperature range, then combustion would continue, exhibiting a very slow, quasi-steady decrease in particle diameter, without runaway. The dashed line itself represents the classical curve of ignition temperature as a function of particle diameter. This line should correspond approximately to the particle-stream experiments of Macek and Semple.[3] For particles approximately 40μ in diameter, their observed ambient temperature at ignition was approximately $T_\infty = 1925$°K, whereas Fig. 7 gives $T_\infty = 1780$°K. Heat loss to the interior of the particle and long ignition times at the tangency condition would tend to make the observed T_∞ exceed the calculated value; thus, the agreement appears to be acceptable. Figure 7

predicts that the ambient temperature required to ignite very small particles in a quasi-steady process is $T_\infty = 1730°K$. For laser ignition, the dashed line is less relevant, and the portions of the solid lines lying above the dashed curve give the temperature above which a particle of a given diameter must be heated to effect ignition in an ambient environment of a specified temperature. It may be seen, for example, that the predicted ignition temperature for a very small particle in room-temperature air is $T_c = 2090°K$.

From the ignition temperature of Fig. 7, the first equality in Eq. (5) can be used in conjunction with Eq. (3) to calculate the thickness h of the oxide film at the ignition condition. The equations imply that h is proportional to d and to the ambient oxygen mole fraction. Use of previous guesses for k and D yields the reasonable value $h = 0.2\mu$ for a 40μ particle in ambient air.

11. Condition for Validity of the Low-Temperature Model

The model developed above is valid only if R_C is less than R_V, the vacuum vaporization rate of B_2O_3(l). A straightforward calculation shows that $R_C/R_V = 2D_a/dc\alpha$, where α is the evaporation coefficient for B_2O_3, and c is the average value of the component of molecular velocity normal to the surface for gaseous B_2O_3 at temperature T_c. Inserting previously employed numbers yields $R_C/R_V \approx (pd\alpha)^{-1}$, with p measured in atmospheres and d in microns. Thus, the model is inapplicable if p or d is too small. The minimum value of the product pd depends on the value of the evaporation coefficient. If $\alpha = 1$, then the model is good for $d \gtrsim 1\mu$ at atmospheric pressure or for $d \gtrsim 100\mu$ at 10^{-2} atm. This encompasses almost all conditions of practical interest. On the other hand, it is possible that α is as low as 10^{-2}, in which case the model requires $d \gtrsim 100\mu$ at atmospheric pressure. This last condition is relatively stringent; if $\alpha = 10^{-2}$, then oxide vaporization is rate controlled in many interesting applications.

If oxide vaporization is rate-controlled, then a different expression must be used for R_C, but otherwise the preceding analysis is unchanged. Equation (12) is no longer valid, but the modified formula for the ignition temperature possesses essentially the same functional dependences, with the exception that the ignition temperature is now predicted to be independent of pressure. This last prediction does not conflict severely with Eq. (12), since the equation predicts roughly a 300°K increase in ignition temperature for a tenfold increase in p.

King[6] cites arguments favoring rate-controlled oxide vaporization under essentially all conditions, including those of Talley.[1,13] Arguments favoring surface equilibrium are the following: Since Talley's tests at atmospheric pressure had $d \approx 1000\mu$, an uncommonly low value of α, approaching 10^{-3}, is needed for Talley's system to be rate-controlled. Talley states[1] that his observed vaporization rate varied inversely with pressure; this is consistent with surface equilibrium and inconsistent with a rate process.

Ignition temperatures calculated by King[6] show a slight decrease with increasing pressure, in contrast with the independence predicted by the corresponding modification of the present analysis. The discrepancy must be traceable to differing definitions of ignition temperature (King's being obtained by carrying on a numerical integration for a certain length of time). King[6] quotes unpublished shock-tube experiments by Uda, in which the ignition temperature was found to decrease with increasing pressure. This observation is in conflict with our model. A careful evaluation of the experimental conditions is needed before the seriousness of the conflict can be established. From the very beginning, progress in studies of boron combustion has been hindered by inadequate publication.

It can be concluded that at sufficiently high values of the product pd, our analysis appears to describe the low-temperature combustion of boron reasonably well. At sufficiently low values of pd the analysis should be modified by employing a kinetically controlled vaporization process for B_2O_3. Where the changeover occurs depends on the value of the evaporation coefficient α.

12. The High-Temperature Stage

We have idealized the equilibrium model of Knipe[4] in order to obtain an analytical expression for the burning rate in the high-temperature stage. The approximate combustion model inferred from Knipe's computations is illustrated in Fig. 8. Although this model enables one to integrate Knipe's governing equations analytically under rather nonstrictive sets of assumptions (e.g., constant but different heat capacities for each species, constant thermal conductivities that may differ on the two sides of the gas-phase flame, diffusion coefficients that are proportional to temperature and that differ for each pair of species), the resulting equations are complicated algebraically. It is simpler and sufficiently accurate to proceed as in Ref. 14. The basic assumptions and the analysis of Ref. 14 can be applied essentially without change to the model illustrated in Fig. 8. The resulting formula for the burning time is

$$t_b = \frac{c_p \rho_l d^2}{8\lambda} \left\{ \ln\left[1 + \frac{QY + c_p(T_\infty - T_l)}{l} \right] \right\}^{-1} \tag{13}$$

where c_p and λ are the specific heat and thermal conductivity of the gas, ρ_l is the density of the liquid boron droplet whose temperature is T_l, T_∞ is the ambient temperature, Y the mass fraction of oxygen in the ambient atmosphere, l is the heat absorbed at temperature T_l in the reaction $B(l) + B_2O_3(g) \rightarrow \frac{3}{2}B_2O_2(g)$ per unit mass of B consumed, and Q is the heat liberated at temperature T_l in the reaction $2B_2O_2(g) + O_2(g) \rightarrow 2B_2O_3(g)$ per unit mass of O_2 consumed.

Estimates indicate that usually radiative losses are unimportant in the second burning stage. We calculate that radiative losses will increase the value of t_b given in Eq. (13) by approximately 10% for $d = 250\mu$. Radiative losses become dominant for $d \gtrsim 1$ mm and negligible for $d \lesssim 100\mu$.

To compare predictions of Eq. (13) with experiment, we assume that $T_l = 2500°K$. As T_l is decreased from this value solidification of boron soon occurs, thereby increasing l and decreasing the burning rate, and shortly thereafter B_2O_3 condenses, placing the system back in the burning regime of the first stage. As T_l increases, the term $c_p T_l$ grows and reduces the burning rate appreciably. Thus our choice of T_l corresponds approximately to the condition of maximum burning rate, which a more thorough analysis that includes dT_l/dt is likely to show to be the correct quasi-steady condition.

For $T_l = 2500°K$, tables[9] imply that $l = 2560$ cal/g and $Q = 5550$ cal/g. As best guesses, which surely will produce better than 30% accuracy in t_b according to our estimates, we employ $c_p = 0.35$ cal/g°K, $\lambda = 3 \times 10^{-4}$ cal/cm sec °K, and $\rho_l = 2.35$ g/cm^3. Burning times so predicted are shown as functions of ambient oxygen concentration and ambient temperature in Fig. 9. Data points of Macek and Semple,[3] plotted on the figure, are seen to be in good agreement with the theory, in absolute value as well as in their dependence on both oxygen concentration and temperature. Macek and Semple[3] reported mean burning times for particles with mean diameters

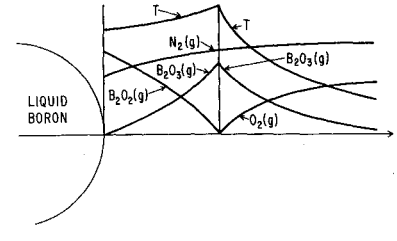

Fig. 8 Model for high-temperature stage in the combustion of boron particles.

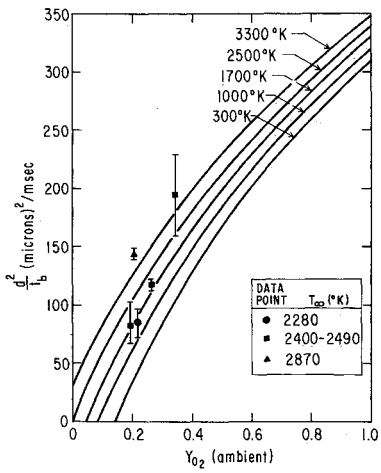

Fig. 9 Burning rate of boron particles, plotted as a function of ambient oxygen concentration, for different ambient temperatures. Solid lines are theory, points average of two (in one case three) experimental average values reported in Ref. 3. Bars indicate extremes of average values reported in Ref. 3.

of 34.5μ (usually the lower limit of vertical bar) and 44.2μ (usually the upper limit of vertical bar); the vertical bars do not represent estimated bounds of experimental error.

It is understandable that the present theoretical results should agree well with the experimental results of Ref. 3, because experimentally the ambient temperature usually exceeded the boiling point of the oxide, thereby assuring the validity of the theoretical approximation that oxide condensation is negligible. To test whether the theory remains accurate in low-temperature environments, we can compare the calculated burning times with those observed for the second combustion stage by Macek and Semple[5] in laser-ignition experiments. The comparisons quoted here will not be precise because of uncertainty in the effective diameter of the particles.[15] In atmospheric air we calculate $t_b = 130$ msec, whereas $t_b = 50$ msec was observed. For pure O_2 the calculated and observed values are 18 and 7 msec, respectively. Also, in air the experimental value of t_b decreased to about 20 msec as the pressure was raised to 35 atm, but no explicit pressure effect appears in the present theory. The observations are all consistent with the presence of significant enhancement of the burning rate by additional heat release associated with gas-phase condensation of B_2O_3—an enhancement that, as expected, increases with increasing pressure. An interesting task for a future simplified model would be to account for gas-phase condensation of B_2O_3, in an effort to achieve better agreement with experiments performed at low ambient temperatures. Unless the ambient temperature exceeds the boiling point of the oxide, the present model over-estimates the burning time, by nearly an order of magnitude in a most extreme case.

13. The Flammability Limit

Setting $t_b = \infty$ in Eq. (13) defines an oxygen concentration below which second-stage combustion should disappear. The predicted limiting oxygen mass fraction is

$$Y_{\text{lim}} = c_p(T_l - T_\infty)/Q = 0.158 - (T_\infty/15{,}800) \qquad (14)$$

which varies from zero at $T_\infty = 2500$°K to 0.139 at $T_\infty = 300$°K. This last value is of the same order as the limit observed by Prentice,[2] but slightly higher, as would be expected if there were an enhancement in Q caused by oxide condensation.

14. Conclusions

Although boron chemistry is more complex than that of many other metals, it appears that the peak temperatures encountered when a boron particle burns are substantially lower than those of a number of other metals of practical interest, such as aluminum. The lower temperatures facilitate the development of combustion models that explain, sometimes quantitatively, existing observations on the ignition and combustion of boron in atmospheres composed of oxygen and inert gases. The models defined in Secs. 7 and 12 are consistent with our observations on the behavior of laser-ignited boron particles, as well as with results of many previously published experiments.

References

[1] Talley, C. P., "Combustion of Elemental Boron," *Aero/Space Engineering*, Vol. 18, June 1959, pp. 37–47.

[2] Prentice, J. L., "Metal Particle Combustion Progress Report, 1 July 1965–1 May 1967," NWC TP 4435, Aug. 1968, Naval Weapons Center, China Lake, Calif.

[3] Macek, A. and Semple, J. M., "Combustion of Boron Particles at Atmospheric Pressure," *Combustion Science and Technology*, Vol. 1, 1969, pp. 181–191.

[4] Knipe, R. H., "Condensed Phase Effects in the Combustion of Boron Particles," Paper WSCI-70-9, April 1970, Western States Section/The Combustion Institute, Berkeley, Calif.

[5] Macek, A. and Semple, J. M., "Combustion of Boron Particles at Elevated Pressures," Project Squid, TR ARC-13-PU, June 1970, Atlantic Research Corp., Alexandria, Va.; also *Thirteenth Symposium (International) on Combustion*, The Combustion Institute, Pittsburgh, Pa., 1971, pp. 859–868.

[6] King, M. H., "Boron Ignition and Combustion in Air-Augmented Rocket Afterburners," *Seventh JANNAF Combustion Meeting*, CPIA Publ. 204, Vol. 1, Feb. 1971, pp. 243–259.

[7] Wilson, R. P. and Williams, F. A., "Experimental Study of the Combustion of Single Aluminum Particles in O_2/Ar," *Thirteenth Symposium (International) on Combustion*, The Combustion Institute, Pittsburgh, Pa., 1971, pp. 833–844.

[8] Hoard, J. L., "Remarks on Structure and Polymorphism in Boron," *Boron-Synthesis Structure and Properties*, Vol. 1, edited by J. A. Kohn, W. F. Nye, and G. K. Gaule, Plenum Press, New York, 1960, pp. 1–6.

[9] *JANAF Thermochemical Tables (Joint Army-Naval-Air Force)*, 1961, Dow Chemical Co., Midland, Nich.

[10] Thompson, J. C. and McDonald, W. J., "Low-temperature Thermal Conductivity of Boron," *Boron-Preparation, Properties and Applications*, Vol. 2, edited by G. K. Gaule, Plenum Press, New York, 1965, pp. 261–267.

[11] Ho, C. Y., Powell, R. W., and Wu, K. Y., "Thermal Diffusivity of the Elements," *Proceedings of the Eighth Conference on Thermal Conductivity*, edited by C. Y. Ho and R. E. Taylor, Plenum Press, New York, 1968, pp. 971–998.

[12] Frenkel, J., *Kinetic Theory of Liquids*, Dover, New York, 1955, pp. 200–208.

[13] Talley, C. P., "The Combustion of Elemental Boron," Progress in Astronautics and Rocketry, Vol. 1," *Solid Propellant Rocket Research*, edited by M. Summerfield, Academic Press, New York, 1960, pp. 279–285.

[14] Williams, F. A., *Combustion Theory*, Addison Wesley, Reading, Mass., 1965, pp. 50–54.

[15] Macek, A., private communication, Dec. 1971.